A reaction norm for flowering time plasticity reveals physiological footprints of maize adaptation

Justine Drouault[1], Carine Palaffre[2], Emilie J. Millet[1], Jonas Rodriguez[1], Pierre Martre[1], Kristian Johnson[1], Boris Parent[1], Claude Welcker[1], Randall J. Wisser[1,3*]

[1]LEPSE, University of Montpellier, INRAE, Institut Agro Montpellier, Montpellier, FR

[2]Experimental Unit of Maize, INRAE, 40390 Saint Martin De Hinx, FR

[3]Department of Plant and Soil Sciences, University of Delaware, Newark, Delaware, USA

***Correspondence:** Randall J. Wisser, randall.wisser@inrae.fr

ORCIDs: EJM: 0000-0002-2913-4892; JR: 0000-0001-8693-1022; PM: 0000-0002-7419-6558; CW: 0000-0002-8275-1259; RJW: 0000-0003-1075-0115

Current address:

Emilie J. Millet: INRAE, UR1052 GAFL, 84143 Montfavet, France

Jonas Rodriguez: Syngenta Seeds, P.O Box 18300, Greensboro, North Carolina, USASyngenta Seeds, P.O Box 18300, Greensboro, North Carolina, USA

keywords: adaptation, common garden trial, envirotyping, flowering time, maize, photoperiod, reaction norm

Running title: Physiological footprints of flowering time adaptation in maize

Date of submission: July 9, 2024

Word count: 4,418

Number of tables and figures

Tables: 2
Figures: 4

Supplementary data

Figures: 2
Files: 6

Abstract

Understanding how plant phenotypes are shaped by their environments is crucial for addressing questions about crop adaptation to new environments. This study investigated the interplay between developmental responses to temperature fluctuations and photoperiod perception in maize that contribute to genotype-by-environment variation in flowering time. We present a physiological reaction norm for flowering time plasticity (PRN-FTP) for studying large collections of genotypes tested in multi-environment trial (MET) networks. Using a new variable for computational envirotyping of sensed photoperiod, it was found that, at high latitudes, different genotypes in the same environment can experience hours-long differences in photoperiod. This emphasizes the importance of considering genotype-specific differences in the experienced environment when investigating plasticity. A statistical framework is introduced for modeling the PRN-FTP as a non-linear response function, with parameters putatively linked to different regulatory modules for flowering time. Applying the PRN-FTP to a sample of global breeding material for maize showed that tropical and temperate maize occupy distinct territories of the trait space for PRN-FTP parameters, supporting that the geographical spread and adaptation of maize was differentially mediated by exogenous and endogenous pathways for flowering time regulation. Our results have implications for understanding crop adaptation and for future crop improvement efforts.

This is a provisional file, not the final typeset article

Introduction

Plants exhibit vast phenotypic diversity, the principal axis for adaptation and evolution. The classic formalism $P = G + E + G \times E$ describes how phenotypes are determined by combinations of genetic (G) and environmental (E) effects. Different environmental conditions can produce distinct phenotypic outcomes for the same genotype, a phenomenon known as plasticity (Bradshaw, 1965). As 21st-century climate markedly shifts the environmental dimension to new frontiers, it is an important and opportune time to investigate mechanisms of environmental plasticity (E) and genetic variation in plastic responses ($G \times E$). Harnessing plastic responses to dominant shifts in climate conditions can facilitate the adaptation of crops into new territories or to alternative cropping systems (Rising and Devineni, 2020; Sloat *et al.*, 2020; Zabel *et al.*, 2021). New approaches for understanding and predicting the responses of traits driven by combinations of climate and weather conditions are also encouraging (Millet *et al.*, 2019; Cooper *et al.*, 2020; van Voorn *et al.*, 2023).

The functional relationship that defines a pattern of phenotypic change across an environmental gradient is known as a reaction norm, which provides information about the direction and magnitude of plasticity (Roof, 1997). To construct norms of reactions, phenotypic values must be recorded in a large number of settings presenting environmental variation, and a relevant variable or index is used to define the gradient of environmental conditions. There are different ways of formulating the response (trait variation) and predictor (environment variation) variables for modeling a reaction norm. Strictly speaking, reaction norms are defined as response functions to single environmental factors, but the term has also been used to describe responses to environments *per se*. A common approach in quantitative genetics uses the *Finlay–Wilkinson* model (Finlay and Wilkinson, 1963), in which the phenotypic values of individual genotypes are regressed on an index defined by the mean values of all genotypes per environment. This method provides a convenient generalization for using multi-environment trials (METs) with large numbers of genotypes to dissect and predict variation in plasticity (Jarquín *et al.*, 2014; Kusmec *et al.*, 2017; Guo *et al.*, 2023). Clearly, however, the environment is abstractly defined, leading to a lack of biological interpretability. In contrast, under controlled settings with fine-scale phenotyping, ecophysiologists have determined response functions of traits to environmental variables that allows for the definition of environmental sensitivities of different plant processes, such as the non-linear response of growth and development to temperature (Parent *et al.*, 2010; Parent and Tardieu, 2012). This provides biological perspective, but upscaling to study broad diversity in METs remains challenging. By extension, crop modelers have tied together these governing principles as mathematical models of ecophysiological processes, leading to systems for predicting the phenotypes of emergent characteristics as a function of genetics and environments (Muller and Martre, 2019). Concepts from these domains can be combined to define and model biologically-informed reaction norms in the design and analysis of MET networks.

In plants, the control of flowering time is regulated by a modular molecular network controlling physiological responses to multiple external signals, particularly temperature and photoperiod (Simpson and Dean, 2002; Colasanti and Coneva, 2009; Blümel *et al.*, 2015; Lee *et al.*, 2021). Responses to temperature occur throughout a plant's life cycle, while the response to photoperiod is growth-stage specific. In maize (*Zea mays* subsp. *mays*), a facultative short-day (SD) species, the stage at which plants become sensitized to photoperiod is not directly observable, but has been found to occur just prior to the timing of tassel initiation for plants grown in SD conditions (Kiniry *et al.*, 1983*a*,*b*). Above a critical photoperiod, tassel initiation is delayed beyond the sensitized stage for photoperiod sensitive genotypes. As physiological responses to temperature fluctuations interact with genotypic variations in the rate and duration and of plant development, different genotypes can reach the sensitized stage on different days, and therefore can perceive different photoperiods, even within

the same environment. For photoperiod sensitive genotypes, genotypic variation in critical thresholds and degrees of photoperiod sensitivity create additional response variation, culminating in the formation of $G \times E$ interactions in flowering time across environments. Extending previous work (Kiniry *et al.*, 1983*a,b*; Choquette *et al.*, 2023), the current study is centered on the modeling and analysis of a physiological reaction norm for flowering time plasticity (PRN-FTP) that captures the combined effects of physiological sensing and responses to temperature and photoperiod underlying variation in flowering time across environments. We formulated this as a bilinear, threshold-dependent function for the relationship between thermal time from crop emergence to male flowering (anthesis; $T_{\mathrm{t}}^{\mathrm{em-ant}}$) and a new environmental index for sensed photoperiod (DL^{s}). We also demonstrate how statistical modeling of the PRN-FTP allows the decoupling of different components of flowering time regulation: (i) flowering time *per se*; (ii) critical photoperiod; and (iii) photoperiod sensitivity.

Constructing PRN-FTPs from METs is the most practical approach for studying flowering time plasticity in large collections of genotypes, but this is difficult due to the geographical structure of photoperiod and the non-linear reaction norm. This requires testing across numerous field sites spanning nearly an entire hemisphere to capture a sufficient range and density of DL^{s} needed to estimate the non-linear function. A better understanding of the variation in DL^{s} within and across environments could aid in the efficient design of METs for studying the PRN-FTP. A particular difficulty is determining critical photoperiods, which in turn affect estimates of flowering time *per se* and photoperiod sensitivity. Also, detecting the true PRN-FTP based on thermal time can be obscured by the influence of other factors besides temperature on growth and development, such as drought (e.g., Harrison *et al*., 2014; Herrero and Johnson 1981). Additionally, since genotypes can become sensitized to photoperiod at different points in time within each environment, it must be considered whether a common reference value or genotype-specific values for DL^{s} should be used for the PRN-FTP. As a result, a full understanding about the diversity of flowering time plasticity in maize and other species has yet to be realized. As another aspect of the current study, new methods are introduced for envirotyping DL^{s} at a global scale, in addition to techniques for statistically analyzing the PRN-FTP.

Even if METs span photoperiod thresholds for a species, sparse coverage of DL^{s} can hinder the ability to fit accurate functions for the PRN-FTP. For instance, an MET network may consist of environments that can only be split into sets of long-day (LD) and SD scenarios by assuming a common threshold for photoperiod sensitivity across all genotypes. In such cases, a simplified LD-SD method may be required, where photoperiod sensitivity is estimated as the difference between mean $T_{\mathrm{t}}^{\mathrm{em-ant}}$ in sets of LD and SD environments (Coles *et al.*, 2010; Hung *et al.*, 2012). In this case, flowering time *per se* can also be estimated as the mean $T_{\mathrm{t}}^{\mathrm{em-ant}}$ among SD environments. Hereafter, this approach is called the LD-SD model.

Finally, parameters of the PRN-FTP may be used to understand how components of flowering time plasticity mediate adaptation to novel environments, and how this in turn changes genotype plasticity for the future. Historical varieties of maize that spread 2000-5000 years ago from their tropical origins into temperate zones required flowering time adaptations to cooler climates with longer photoperiods (Tenaillon and Charcosset, 2011). Using the LD-SD method for genetic dissection, selection on genes controlling photoperiod sensitivity have been identified as key factors for the tropical-to-temperate transition of maize (Hung *et al.*, 2012; Yang *et al.*, 2013). Varieties adapted to temperate zones have effectively lost their sense of photoperiod, such that flowering times are largely determined by temperature interactions with variation in flowering time *per se*. Similar results from the adaptation of tropical populations to temperate environments have been observed over short timescales (within 10 generations). When tropical populations have been selected for early flowering time in LD temperate environments, photoperiod sensitivity was found to rapidly diminish while flowering time *per se* was

This is a provisional file, not the final typeset article

gradually reduced (Teixeira *et al.*, 2015; Wisser *et al.*, 2019; Choquette *et al.*, 2023). In contrast, selection in SD environments reduced only flowering time *per se*, since photoperiod sensitivity was not induced (Choquette *et al.*, 2023). Here, we show that relating the variation in flowering time *per se* and photoperiod sensitivity for separate breeding pools can be used to understand how selection history has shaped the plasticity of modern maize.

Materials and Methods

Experimental datasets

Multiple experiments and datasets from different projects were assembled to: (D1) select a temperature response function for thermal time estimation; (D2) estimate the thermal time duration between crop emergence and tassel initiation ($T_{\mathrm{t}}^{\mathrm{em-TI}}$) for diverse maize lines; (D3) envirotype sensed photoperiod (DL^{s}) in maize fields across the Northern Hemisphere; (D4) demonstrate methods for modeling a physiological reaction norm for flowering time plasticity (PRN-FTP); and (D5) compare the trait space of parameters estimated from the PRN-FTP in a diversity panel constituting separate breeding pools of maize. The current study focuses on days to anthesis (male flowering) as the final characteristic.

(D1) Three temperature response functions (Methods S1, Eq. S1-S3) for measuring thermal time were compared using a dataset with 19 hybrids tested in at least 34 field environments, spanning latitudes from 30.5371°N to 51.5016°N (File S1; data sourced from the Genomes-To-Fields Initiative). For each environment, the sowing date, field coordinates, and best linear unbiased estimates (BLUEs) for calendar days from planting to anthesis were obtained from McFarland *et al*., 2020 and Rogers *et al*., 2021. Using temperature data, the genotype-specific BLUEs for calendar days to anthesis were converted to thermal time values.

(D2) The $T_{\mathrm{t}}^{\mathrm{em-TI}}$ was estimated for a collection of 239 maize inbred lines (panel 1) using a physiological formalism (Eq. 1), based on data for crop emergence, phyllochron, and final leaf number recorded in two experiments under short-day (SD) conditions (File S2). The $T_{\mathrm{t}}^{\mathrm{em-TI}}$ measured in SD conditions is referred to as the basic vegetative phase to tassel initiation (BVP-ti; Kiniry *et al.*, 1983*a*). Panel 1 primarily consisted of semi-tropical or tropical lines but included some temperate lines. Crop emergence and phyllochron were measured in a greenhouse phenotyping platform at the LEPSE of INRAE (PhenoArch, Montpellier, FR; Cabrera-Bosquet *et al.*, 2016) under well-watered conditions, while final leaf number was recorded in a field experiment in Puerto Vallarta, MX, also in well-watered conditions. For both experiments, daylengths throughout the growth cycle never exceeded 12.5 h, providing SD conditions in which photoperiod was not expected to suppress tassel initiation. Additional details for these experiments can be found in Supplemental Information (Methods S2).

(D3) Using the BVP-ti as a proxy for DL^{s}, computational envirotyping of DL^{s} was performed for fields across the Northern Hemisphere (latitudinal range of 13.7578 °N to 54.2900 °N) where maize was previously grown. For this, the geographical coordinates and planting dates of 680 field environments were assembled from past publications and ongoing projects (File S3). Crop emergence dates available from 15 field environments sourced from the Maize ATLAS project (Choquette *et al.*, 2023) were used to compute a mean thermal time from sowing to emergence of 76 °Cd (estimated using Eq. S2), which was used for predicting times to emergence in the remaining environments where only the planting date was available.

(D4) To test modeling procedures for the PRN-FTP, flowering time data from 37 field trials were combined into a multi-environment trial (MET) dataset (File S4). The dataset included observations

that maximized observations for a common set of genotypes also present in dataset D2, including seven temperate inbred lines (B37, B73, M37W, Mo17, Oh43, LH123Ht, and 2369) and seven tropical inbred lines (CML10, CML258, CML277, CML341, CML373, Tzi8, and Tzi9). Still, representation of these lines across the 37 environments was not fully balanced. The temperate lines were present in a minimum of 13 and a maximum of 22 environments. The tropical lines were present in a minimum of 18 and a maximum of 37 environments.

(D5) To examine the relationship between PRN-FTP parameters associated with flowering time *per se* and photoperiod sensitivity, MET data for a collection of 111 temperate, 52 tropical, and 51 admixed inbred lines constituting separate breeding pools (panel 2; Flint-Garcia *et al*., 2005) was assembled from previous experiments (File S5). These lines were observed across a maximum of three SD environments (maximum photoperiod <12.3 h) and 16 long-day (LD) environments (minimum photoperiod of >14.5 h) spanning 18.00 °N to 42.76 °N latitude.

Environmental data

For field trials considered in this study, temperature data were acquired from ground and satellite data sources for a common reference point of 2 m height. Ground data were obtained mostly from weather stations at a given field location. In two cases, ground data from a nearby airport within 5 km of the experimental field site was obtained from Weather Underground (https://www.wunderground.com/). Satellite data (weather variable 'T2M'; spatial resolution of ½° latitude x ⅝° longitude) was acquired from the R package *nasapower* (Sparks, 2018) using the latitude and longitude coordinates for each field location.

The photoperiod based on civil twilight at a given location for a given day of the year was acquired from the R package *TrenchR* (Buckley *et al.*, 2023). This uses the CBM daylength model described by Forsythe *et al.* (1995).

Comparison of temperature response functions

Three temperature response functions were compared for calculating thermal time (Eq. S1-S3). Comparisons were made based on the normalized root mean square error (NRMSE, normalized by the difference between maximum and minimum values) for the overall mean thermal time from sowing to anthesis. The NRMSE was estimated for each of the 19 hybrids in dataset D1 in order to identify the response function that minimized the mean NRMSE among all hybrids. The analyzed set of hybrids were from crosses between temperate-adapted lines classified as photoperiod insensitive, such that variation in anthesis dates (calendar days) across environments were expected to be primarily due to differences in temperature. Therefore, the magnitude of residual variation per hybrid was expected to reflect deviations from the model for temperature response. For the purpose of comparing different models for thermal time estimation, we assumed the influence of any latent variables on growth and development could be ignored.

Physiological reaction norm for flowering time

The PRN-FTP defined here was reformulated from a previous model by Kiniry *et al.* (1983*a*) that described the relationship between photoperiod conditions (x-axis) and thermal time from crop emergence to tassel initiation ($T_{\mathrm{t}}^{\mathrm{em-TI}}$; y-axis). Kiniry *et al.* (1983*a*) used growth chambers in which constant levels of photoperiod were applied throughout the plant's growth cycle. However, in the setting of MET networks considered here, photoperiods are not constant (DL^{s} depends on the timing at which a plant become sensitized to photoperiod in a given environment) and estimating tassel

This is a provisional file, not the final typeset article

initiation from dissections of the shoot apical meristem is not practical at large scale (rather, in METs, days to flowering are routinely recorded). Since there is no visible marker for when DL^s occurs, we devised a proxy measure based on previous results showing that the initial stage of sensitization to photoperiod closely corresponds to the BVP-ti (i.e., the $T_{\mathrm{t}}^{\mathrm{em-TI}}$ measured under SD conditions; Kiniry *et al.*, 1983*b*). Thus, here we define the PRN-FTP as the relationship between the proxy measure for DL^s (x-axis) and thermal time from crop emergence to anthesis ($T_{\mathrm{t}}^{\mathrm{em-ant}}$; y-axis)

DL^s was obtained by first calculating $T_{\mathrm{t}}^{\mathrm{em-TI}}$ (Eq. 1) for genotypes grown in SD conditions (Methods S2). Considering that tassel initiation occurs on the day when the last leaf primordium is formed (Lejeune and Bernier, 1996) and that rates of leaf primordia formation and leaf tip appearance are proportional, $T_{\mathrm{t}}^{\mathrm{em-TI}}$ can be calculated as:

$$T_{\mathrm{t}_i}^{\mathrm{em-TI}} = \frac{P_{\mathrm{tip}_i}}{\alpha_{\mathrm{phyll/plast}}}\left(L_{\mathrm{F}_i} - L_{\mathrm{pri}}^{\mathrm{em}}\right) \qquad \text{(Eq. 1)}$$

where, $T_{\mathrm{t}_i}^{\mathrm{em-TI}}$ (°Cd) is the cumulative thermal time from crop emergence to tassel initiation of the ith genotype, P_{tip_i} (leaf °Cd^{-1}) is the phyllochron of the ith genotype (i.e., the thermal time between the appearance of two successive leaf tips), L_{F_i} (leaf) is the final leaf number of the ith genotype, $\alpha_{\mathrm{plast/phyll}}$ (dimensionless) is a constant ratio of phyllochron to plastochron (i.e., the thermal time between the formation of two successive leaf primordia), and $L_{\mathrm{pri}}^{\mathrm{em}}$ (primordium) is a constant number of primordia formed at crop emergence. Genotype-specific values for P_{tip_i} and L_{F_i} were obtained from dataset D2 on panel 1 (Methods S2). For maize, $\alpha_{\mathrm{plast/phyll}}$ may range from 1.58 to 1.85 (Kiniry, 1991; Lejeune and Bernier, 1996; Padilla and Otegui, 2005; Andrieu *et al.*, 2006). In this study, we set it at the average value reported in the literature (1.73). There are four to five leaf primordia in the embryo of maize seeds (Bonnett, 1954; Padilla and Otegui, 2005) and between germination and crop emergence about two other leaf primordia are formed (Padilla and Otegui, 2005). Here, $L_{\mathrm{pri}}^{\mathrm{em}}$ was set equal to 5.5 primordia.

Finally, given a sowing date, the thermal time from sowing to crop emergence, and the $T_{\mathrm{t}}^{\mathrm{em-TI}}$ from Eq. 1, the temperature records for each environment were used to predict the calendar day that a given genotype becomes sensitized to photoperiod. In turn, the photoperiod of the specific calendar day in that environment was predicted using the R package *TrenchR* (Buckley *et al.*, 2023) to obtain the DL^s.

Envirotyping of sensed photoperiod

Dataset D3 was used to computationally envirotype DL^s for maize across cultivation areas in the Northern Hemisphere. In addition, differences in DL^s were quantified for three maturity groups, defined by the lower (5th), median (50th), and upper (95th) percentiles of the $T_{\mathrm{t}}^{\mathrm{em-TI}}$ distribution estimated for panel 1 (Table 1). The thermal time from sowing to crop emergence (fixed value based on mean from observations in D3), plus the percentile-maturity group value of $T_{\mathrm{t}}^{\mathrm{em-TI}}$ was used to predict corresponding DL^s values per environment. In each environment, the rate of photoperiodic change was also computed between single days flanking the day of DL^s for the 50th percentile-maturity group.

In a typical application, the PRN-FTP would be constructed for each of the genotypes tested in the MET. While $T_{\mathrm{t}}^{\mathrm{em-ant}}$ are specific to the observations on each genotype, the DL^s could be defined for each specific genotype or a common reference genotype. The choice depends on whether different genotypes in the same environment experience large or small differences in photoperiod. Therefore, a

257 sensitivity analysis was performed to assess the impact of using genotype-specific values versus a
258 common reference value for DL^s.

259 **Statistical analysis of the PRN-FTP**

260 With a sufficient coverage of DL^s spanning SD and LD environments, we modeled the PRN-FTP using
261 a continuous two-phase (bilinear) regression model with threshold detection (Fong *et al.*, 2017*a*). Here,
262 using the R package *chngpt* (Fong *et al.*, 2017*b*), the "hinge model" was fit to the PRN-FTP for each
263 genotype in dataset D4.

264 $$T_{\mathrm{t}}^{\mathrm{em-ant}} = \alpha + \beta(DL^s - e)_+ \qquad \text{(Eq. 2)}$$

265 where $T_{\mathrm{t}}^{\mathrm{em-ant}}$ is the response variable; e is the threshold parameter; DL^s is the sensed daylength with
266 a threshold effect; $I(DL^s > e) = 1$ when $DL^s > e$ and 0 if $DL^s \leq e$; $(DL^s - e)_+$ denotes the hinge
267 function, which equals $DL^s - e$ for $DL^s > e$ and 0 otherwise; and α and β are the intercept and slope
268 parameters, respectively . The model was fitted using default settings, with no constraints set for
269 estimating the threshold value (breaking point of the bilinear model). Estimated effects include an
270 intercept, threshold value, and slope, which correspond to physiological components of flowering time:
271 the flowering time *per se*, the critical threshold for photoperiod sensitivity, and the degree of
272 photoperiod sensitivity, respectively.

273 *Correction for latent variables affecting thermal times to anthesis*. If only temperature influenced the
274 flowering time of a photoperiod insensitive genotype, their $T_{\mathrm{t}}^{\mathrm{em-ant}}$ would be nearly the same across
275 an MET. In our experience, this simplistic assumption often does not hold (as confirmed with dataset
276 D1), but the cause for deviations can be due to various possibilities, including the influence of other
277 environmental factors, differences in crop management practices, differences between air temperature
278 and the temperature sensed by the crop, imprecision and biases in weather data, or other latent
279 variables. Therefore, with dataset D4, we tested an alternative approach using photoperiod insensitive
280 control lines to adjust for across environment latent variable effects prior to constructing the PRN-FTP.

281 Seven photoperiod insensitive temperate genotypes were defined as control lines. The 37 environments
282 for dataset D4 were assembled from different experiments but unfortunately did not include all seven
283 control lines in all environments, so two sets of control groups were defined (set 1: B37, B73, M37W,
284 Mo17, and Oh43; set 2: LH123Ht and 2369). Sets 1 and 2 were associated with 22 and 13 of the
285 environments, respectively. For each set, the overall mean of $T_{\mathrm{t}}^{\mathrm{em-ant}}$ was calculated across
286 environments of the MET in which they were associated. The environment-specific residuals were then
287 used to adjust the thermal times for the remaining non-control genotypes in each of the corresponding
288 environments of the MET. We note that using two sets of control lines that were also imbalanced across
289 environments (see above) could introduce some bias and is not ideal, but our aim was to test this
290 approach.

291 **Analysis of flowering time plasticity in a diversity panel**

292 We sought to investigate the relationship between flowering time *per se* and photoperiod sensitivity in
293 panel 2 (dataset D5). The MET lacked sufficient coverage of DL^s to estimate critical threshold values
294 for the PRN-FTP using the hinge model. Therefore, the parameters were estimated by an LD-SD
295 method using simple linear regression of the BLUEs for $T_{\mathrm{t}}^{\mathrm{em-ant}}$ (response variable) on the means of
296 the DL^s values for the set of SD (range of 11.9 h to 12.3 h) and LD (range of 15.4 to 16.0 h)
297 environments (predictor variable). Not all genotypes were observed in all environments. Therefore,

This is a provisional file, not the final typeset article

DL^s means used for regression analysis varied slightly by genotype according to the sets of environments for which data were available. When fitting the LD-SD linear regression model, the DL^s means were offset to zero so that the intercept was estimated at the mean short-day index for the corresponding genotype. The degree of photoperiod sensitivity was determined as the slope of the regression.

Results

Choosing a temperature response function to construct the PRN-FTP

Thermal time is used in the estimation of DL^s for envirotyping and formulating the PRN-FTP function, such that the choice of a temperature response function could result in different outcomes. A comparison of different temperature response functions showed no difference in the NRMSEs for thermal times to anthesis for 19 photoperiod-insensitive hybrids tested in more than 34 environments in North America. Regardless of the temperature response function that was tested, for each hybrid, the environment-specific thermal time to anthesis deviated, on average, by ~10% (range 7 to 12%) from the across-environment mean (Fig. S1). Therefore, for the current study, we chose the non-linear response function by Wang and Engel (1998) adapted for maize (Eq. S2) due to its common implementation in crop growth models (Wang *et al.*, 2017), its higher physiological realism compared with the linear response function (Eq. S1), and its greater flexibility compared to the Arhenus model proposed by (Eq. S3; Parent *et al.*, 2010).

Predicting when maize becomes sensitized to photoperiod

There is no known visible marker to measure the timing when maize plants become sensitized to photoperiod. Here, we defined this timing using $T_{\mathrm{t}}^{\mathrm{em-TI}}$ measured under SD conditions since this closely corresponds to the photoperiod sensitized phase (Kiniry *et al.*, 1983*b*). An issue is that directly observing tassel initiation requires temporal dissections of shoot apical meristems which is not possible at a large scale. To circumvent this, we used an ecophysiological formalism to predict genotype-specific values for $T_{\mathrm{t}}^{\mathrm{em-TI}}$ (Eq. 1) in panel 1 grown under SD conditions (dataset D2; File S2). A summary of the variation in $T_{\mathrm{t}}^{\mathrm{em-TI}}$ is shown in Table 1. In a separate experiment, using a phenotyping platform with a constant 11 h photoperiod, longitudinal dissections of shoot apical meristems were performed on eight of the lines from the same panel (Methods S2). The Pearson correlation coefficient between the shoot apical meristem transition and the predicted BVP-ti was 0.70, indicating the formalism-based predictions for $T_{\mathrm{t}}^{\mathrm{em-TI}}$ were reasonably approximated.

Variation in the sensed photoperiod for maize

DL^s integrates information on sowing dates, emergence dates, developmental responses to temperature, the temperature and photoperiodic conditions of an environment, and the genetic diversity for the physiological traits underlying flowering time. This can be used to understand how different genotypes sense photoperiod within and across environments, and how it varies according to spatiotemporal patterns in climate and weather. To examine how photoperiods are perceived by maize, we computationally envirotyped DL^s for 680 field environments across the Northern Hemisphere where maize has been previously grown (Fig. 1).

We first summarized the spatial axis of variation in DL^s using the 50th percentile of $T_{\mathrm{t}}^{\mathrm{em-TI}}$ (319 °Cd) in panel 1 as a common reference for envirotyping (Table 1; Fig. S2). The maximum difference in DL^s among all of the environments was 6.4 hours (range: 11.9 to 18.3 h; Fig. 1a). This was primarily driven

339 by climatic variation in photoperiod across latitude and seasonality for maize cultivation. Temperature
340 variation and different sowing dates across years at the same planting location or fields at similar
341 longitudes also led to differences in DL^s, but to a lesser extent. Among 125 field sites where maize was
342 planted for at least two years, DL^s varied by as much as 1.7 hours, with a mean difference of 0.41 h.
343 Similarly, considering a 5-degree band of latitude covering -105° to 5° E longitude, traversing maize
344 fields from the USA and Europe, DL^s ranged from 14.9 to 16.7 h, a difference of 1.8 h.

345 Next, we questioned the extent to which multiple genotypes grown within the same field environment
346 perceive a different photoperiod. Beyond the equator, photoperiod is not constant across days of the
347 year, with increasing rates of daily change in association with latitude. Therefore, genotypes differing
348 in their $T_{\mathrm{t}}^{\mathrm{em-TI}}$ will reach their photoperiod sensitized stage on different days and hence perceive a
349 different photoperiod (Fig. 1b-c), but to our knowledge the extent to which this varies has not been
350 investigated. Using the 5th (236 °Cd) and 95th (430 °Cd) percentiles of $T_{\mathrm{t}}^{\mathrm{em-TI}}$ in panel 1 to represent
351 early and late percentile-maturity groups, the DL^s at these limits frequently differed by more than 1 h,
352 with the largest difference reaching 3.4 h (Fig. 1b). Differences in DL^s above 2 h were rare and occurred
353 only at high latitudes where late genotypes are not cultivated for maize production. Nevertheless, this
354 highlights how the genetic diversity of maize can intersect with environmental variation within the
355 same field, leading to differences in the photoperiod to which genotypes respond.

356 Considering the use of the 50th percentile as a common reference for all genotypes, the relative
357 difference in DL^s for early and late percentile-maturity groups varied by as little as no difference to as
358 much as 1.35 h and 2.04 h, respectively (File S3). The largest differences in DL^s among genotypes
359 within the same field occurred at high latitudes where rates of photoperiodic change were greatest. This
360 reduced to zero as a function of the rate of photoperiodic change (Fig. 1d).

361 **Using METs for modeling the PRN-FTP**

362 To demonstrate and test approaches for modeling the PRN-FTP, we combined flowering time data
363 from multiple experiments into an MET (dataset D4) for a common set of seven genotypes of tropical
364 origin that were expected to be photoperiod sensitive. This was used to estimate the flowering time *per*
365 *se* (intercept), the critical photoperiod (threshold), and the photoperiod sensitivity (slope) using a two-
366 phase regression model (see methods; Fig. 2).

367 Since different genotypes can experience different photoperiods across common environments, we
368 tested the impact of using values of DL^s estimated from a common reference (i.e., the 50th percentile
369 of $T_{\mathrm{t}}^{\mathrm{em-TI}}$ in panel 1) versus separate, genotype-specific values when constructing the PRN-FTP.
370 Compared to the common reference, the $T_{\mathrm{t}}^{\mathrm{em-TI}}$ values used for estimating DL^s ranged from the 37th
371 to 95th percentiles of the $T_{\mathrm{t}}^{\mathrm{em-TI}}$ distribution in panel 1. Comparing DL^s values across the MET of
372 dataset D4, the photoperiods perceived by specific genotypes relative to the common reference differed
373 by no more than 0.47 h. In this case, there was no change in the estimated thresholds for sensitivity
374 and differences in the coefficient estimates were negligible.

375 Using MET data to construct the PRN-FTP makes the simplistic assumption that physiological
376 sensitivities to temperature and photoperiod are the only environmental factors influencing flowering
377 time. Although temperature and photoperiod are dominant factors, other variables can also affect maize
378 growth and development, but the specific causes are often unknown and likely to vary from one
379 environment to another. Therefore, we devised an approach to control for this. Using a set of
380 photoperiod insensitive genotypes present in the same MET, their overall mean $T_{\mathrm{t}}^{\mathrm{em-ant}}$ was defined
381 as an expected value for the common effect of temperature across environments (i.e., for photoperiod

This is a provisional file, not the final typeset article

382 insensitive genotypes, T_t^{em-ant} is expected to be the same across environments, with deviations
383 attributed to latent variables; see Materials and Methods). Next, environment-specific deviations from
384 the overall mean of the insensitive lines were used to adjust the observed T_t^{em-ant} for the remaining
385 lines in each of the corresponding environments. Fig. 2 portrays this procedure and how it affects
386 estimates for the PRN-FTP parameters.

387 When tested on the set of seven tropical genotypes, using adjusted values led to changes in the
388 estimated thresholds of sensitivity, which in turn resulted in differences in the estimated flowering
389 times *per se* and slopes of sensitivity (Table 2). On average, latent variable adjustment enhanced the
390 precision of the overall model fit of the PRN-FTP for each genotype by two-fold (Table 2). Even for
391 this small sample of genotypes, Fig. 3 highlights the diversity of flowering time plasticity in maize
392 consisting of unique parameterizations of the PRN-FTP.

393 **Relating components of the PRN-FTP to understand maize adaptation**

394 Since flowering time *per se* and photoperiod sensitivity underlie flowering time adaptation across
395 environments (Choquette *et al.*, 2023), we questioned how these PRN-FTP components differ between
396 primary breeding pools of maize. For this, we assembled an MET dataset (D5) from 19 field trials with
397 a common set of inbred lines consisting of tropical, temperate, and admixed breeding material.
398 Computational envirotyping showed that DL^s for this MET was restricted to two small intervals of
399 photoperiod conditions, with three environments of 11.9 to 12.3 h photoperiod and 16 environments
400 of 14.5 to16.5 h photoperiod. With a large gap in coverage of DL^s, the two-phase regression function
401 for the PRN-FTP could not be reliably fit. In this case, the PRN-FTP was modeled using an LD-SD
402 method based on simple linear regression after adjusting for latent variables. Examining the
403 relationship between flowering time *per se* and photoperiod sensitivity parameters of the PRN-FTP
404 showed that temperate and tropical material occupy distinct territories of the trait space (Fig. 4; File
405 S6). Temperate lines tend to have a lower flowering time *per se* and nearly no photoperiod sensitivity,
406 while tropical lines tend to have a higher flowering time *per se* coupled with moderate to high degrees
407 of photoperiod sensitivity. Fitting expectations, genotypes with admixed ancestry are positioned
408 between the two.

409 **Discussion**

410 Understanding trait plasticity is important for adapting crops to new environments. To study the
411 variation in plastic responses, METs allow large collections of genotypes to be characterized across
412 environmental gradients. However, due to phenological variation and stage-specific sensitivities,
413 different genotypes within each environment do not experience identical environmental conditions
414 (e.g., Millet *et al.*, 2019). This complicates the definition of environmental indices for modeling
415 reaction norms from METs, challenging standard approaches that assume a common environment is
416 sensed by all genotypes. Based on the ecophysiology of maize flowering time, the current study defines
417 a new, genotype-specific metric for quantifying the photoperiod sensed by diverse genotypes within
418 and across environments. Using DL^s to envirotype maize fields in the Northern Hemisphere, we
419 showed that, at high latitudes, where cooler temperatures that slow development combine with
420 relatively large daily rates of photoperiodic change, genotypes in the same environment can experience
421 more than a 1 h difference in DL^s (Fig. 1). Thus, to provide more accurate information about the
422 variation in trait plasticity, the construction of genotype-specific PRNs for flowering time and other
423 traits should be considered. Assembling several experiments, we also found that MET datasets for
424 maize have limited to no coverage of DL^s from 12.5 to 14.0 h for characterizing variation in critical
425 thresholds for the photoperiod sensitivity of maize. With scant information on variation in critical

426 photoperiods, and given the dependence of accurate threshold estimation for regression analysis of the
427 PRN-FTP (Table 2), envirotyping with DL^s can be used to strategically sample environments for more
428 efficient designs of new METs.

429 The PRN-FTP provides a parsimonious model for flowering time plasticity, taking into account the
430 dominant effects of temperature and photoperiod. However, in METs, additional latent variables can
431 affect flowering time, requiring appropriate adjustments. To address this issue, we applied a between-
432 environment covariate adjustment using photoperiod-insensitive control lines that were expected to
433 have the same thermal time to anthesis across the full range of DL^s. This resulted in a more precise fit
434 of the bilinear response function for the PRN-FTP (Table 2; Fig. 2). Nevertheless, it is important to
435 acknowledge that the choice of a control group could introduce some bias, as it may uniquely vary in
436 other ecophysiological responses. Another challenge in modeling the PRN-FTP is that not all
437 genotypes exhibit a clear bilinear response. For example, photoperiod-insensitive genotypes only
438 display differences in flowering time *per se*, rendering the two-phase regression function invalid. In
439 such cases, linear regression using the LD-SD method is the most appropriate way of capturing the
440 relationship between $T_{\mathrm{t}}^{\mathrm{em-ant}}$ and DL^s. Thus, while the PRN-FTP model offers a valuable framework
441 for understanding flowering time plasticity, careful consideration of latent variables, choice of control
442 group, and genotype-specific responses is necessary for accurate modeling. Incorporating additional
443 factors and exploring alternative models may further improve the utility of the PRN-FT model for
444 applications in plant science.

445 A large body of work has elucidated a generally conserved molecular network for flowering time
446 regulation in plants, involving a set of semi-independent pathways that converge on the genetic control
447 of shoot apical meristem identity and anthesis date (Srikanth and Schmid, 2011; Dong *et al.*, 2012). In
448 several crops including maize, there has been significant progress in understanding the multigenic
449 architectures for variation in days to flowering time and photoperiod sensitivity, reflective of the
450 complex network structure of flowering time regulation. We propose that constructing and
451 decomposing the PRN-FTP from METs on large collections of genotypes can be used to unravel the
452 variation linked to some of these specific pathways. Estimates for critical photoperiods and photoperiod
453 sensitivities from the PRN-FTP can be expected to capture interaction variation between the circadian
454 clock and the photoperiod response pathways (Itoh *et al.*, 2010), along with the possible partial effects
455 of the gibberellic acid pathway suggested by some observations (Johansson and Staiger, 2015; Izawa,
456 2021). Correcting for latent variables should remove some of the effects of other environment-
457 dependent responses that influence flowering time, leading to more accurate estimates of the variation
458 in the photoperiodic responses. We expect that flowering time *per se* primarily reflects endogenous
459 pathways including the autonomous, aging, and gibberellic acid pathways, whereby flowering time is
460 regulated independent of daylength (Minow *et al.*, 2018). The use of thermal time, however, negates
461 the analysis of variation arising from temperature effects, which is an emerging pathway in the
462 regulation of flowering time (Lee *et al.*, 2013; Jin *et al.*, 2023).

463 Predating the advent of modern varieties, populations of maize expanded from their tropical origins
464 into temperate zones (Tenaillon and Charcosset, 2011; Swarts *et al.*, 2017). This was facilitated by
465 flowering time adaptations, evidenced by selection on separate modules of the gene regulatory network
466 for flowering time (Gaudinier and Blackman, 2020). Distinct breeding pools for maize were then
467 established from locally preadapted populations, which have largely persisted as separate pools of
468 tropical and temperate maize. Thus, we reasoned that the PRN-FTP trait space of photoperiod
469 sensitivity and flowering time *per se* for modern varieties could be used to infer about historical
470 selection on flowering time pathways in maize. Figure 4 corroborates that distinct selection on these
471 pathway-associated components of flowering time have structured the plasticity of tropical and

This is a provisional file, not the final typeset article

472 temperate maize. However, the overall trend of reducing photoperiod sensitivity with flowering time
473 *per se* is not necessarily indicative of genetic or physiological coupling of the regulatory pathways,
474 such that genotypes with short flowering time *per se* and high photoperiod sensitivity could exist.
475 Instead, this appears to be a byproduct of the preadaptation history and subsequent breeding of maize.
476 This is supported by results from experimental evolution for early flowering time in tropical
477 populations where photoperiod sensitivity is rapidly eliminated while flowering time *per se* is
478 continually shortened by selection in LD environments of the temperate zone (Teixeira *et al.*, 2015;
479 Choquette *et al.*, 2023). In contrast, selection in SD environments of the tropical zone has no effect on
480 photoperiod sensitivity, where the longer growing seasons have limited the selection for a reduced
481 flowering time *per se*. This highlights how the PRN-FTP can be used for studying crop diversity, and
482 that knowledge about the historical context of adaptation and breeding is crucial for interpreting the
483 observed patterns in the PRN-FTP-derived trait space.

484 **Conclusions**

485 In this study, we explored various aspects of a physiological reaction norm for modeling flowering
486 time plasticity in maize. Envirotyping with DL^s is a valuable tool for examining the global distribution
487 of DL^s in maize and for designing structured METs to investigate the diversity of components of the
488 PRN-FTP. Notably, current MET data is sparse which makes it difficult to characterize the variation
489 in critical thresholds for maize, warranting further experimentation.

490 The PRN-FTP model provides an ecophysiological framework for understanding (GxE) variation in
491 flowering time. For a specific genotype, the pace of development towards reproductive transition is
492 affected by temperature fluctuations within an environment, with the magnitude of this influence
493 varying across environments based on the unique temperature patterns. When contrasting genotypes
494 are present in the same environments, interactions between temperatures and genetic variation in rates
495 of development and $T_{\mathrm{t}}^{\mathrm{em-TI}}$ gives rise to variation in the timing of photoperiod sensitization. In turn,
496 genetic variation in critical thresholds and photoperiod sensitivities lead to secondary interactions with
497 daily rates of photoperiodic change within and across environments. In essence, as genotypes become
498 sensitized to photoperiod at different times, genetic variation in their response to photoperiod further
499 alters the timing of reproductive transition and flowering time, whether or not they are exposed to the
500 same photoperiod within an environment. This highlights the intricate interplay between genetic and
501 environment effects that shape the complex trait variation of flowering time.

502 Lastly, as the PRN-FTP model is based on common ecophysiological processes, we expect that it can
503 be extended to other crops. Investigating the trait space of PRN-FTP components can provide valuable
504 insights into flowering time adaptations in various species. Our findings underscore the significance of
505 considering the historical context of adaptation and breeding in unraveling the genetic and
506 physiological underpinnings of complex traits. This, in turn, holds promising implications for future
507 crop improvement endeavors.

508 **Acknowledgements:** This study was made possible thanks to the production and availability of
509 datasets from prior and ongoing projects: the EXPOSE and PhotoGrid projects at INRAE-LEPSE
510 (ANR-16-IDEX-0006; France 2030 program; Post AgreenSkills Fund), the INVITE project (European
511 Union's Horizon 2020 research and innovation program, grant no. 817970), the Maize ATLAS project
512 (USDA-ARS, grant no. 2011-67003-30342), the Multiple Disease Resistance project (North Carolina
513 State University, Cornell University, and University of Delaware collaboration), the Genomes-to-
514 Fields Initiative (https://www.genomes2fields.org/home/), and the Panzea project (NSF-PGRP, grant

no. 1238014). We wish to thank a number of people who contributed to this study: (i) Mainassara Abdou Zaman-Allah, Terence Molnar, and Prasanna Boddupalli from CIMMYT for providing much of the germplasm used for panel 1; (ii) Alexis Bédiée, Llorenç Cabrera-Bosquet, Nicole Choquette, Arnaud Desbiez-Piat, Thomas Laisné, Noé Lalouette-Marrier d'Unienville, Maëlle Lis, Anthony Rosello, Javier Soto Mendoza, and Benoît Suard for supporting the PhenoArch platform experiments at Montpellier, FR; (iii) Arnaud Brunet, Bernard Lagardere, and Jean-Rene Loustalot from the experimental station at Saint-Martin-de-Hinx, FR for supporting germplasm management and field testing; (iv) the ISRA team Ibrahima Sarr, Malick Ndiaye, Awa Mbengue, Abdoulaye Hoth, and Alain Audebert (CIRAD) for field trial data from Nioro du Rip, SN; and (v) the Moreno Retis team José Moreno and Luis Rodríguez for field trial data from Puerto Vallarta, MX.

Author Contributions: JD, RJW: conceptualization; CP, CW, RJW: resources; JD, CP, EM, RJW: investigation; JD, CP, JR, RJW: data curation; JD, PM, BP, RJW: methodology; JD, JR, KJ, RJW: formal analysis; JD, RJW: writing - original draft; EM, JR, PM, KJ: writing - review & editing; BP, CW, RJW: supervision; EM, RJW: funding acquisition.

Conflict of Interest: The authors declare that the research was conducted in the absence of any commercial or financial relationships that could be construed as a potential conflict of interest.

Funding Statement: This work was supported by the French National Research Agency (ANR-16-IDEX-0006), the France 2030 program, project EXPOSE (PAF_18) supported by INRAE, and the European Union's Horizon 2020 research and innovation program, grant no. 817970.

Data Availability: Data and metadata from this study are available in Supplementary Files at Dryad (https://doi.org/10.5061/dryad.x95x69pth). Sources of external data are indicated in the methods sections. Code for fitting the PRN-FTP is available at: https://github.com/maizeatlas/prnftp.

This is a provisional file, not the final typeset article

References

Andrieu B, Hillier J, Birch C. 2006. Onset of sheath extension and duration of lamina extension are major determinants of the response of maize lamina length to plant density. Annals of Botany **98**, 1005–1016.

Blümel M, Dally N, Jung C. 2015. Flowering time regulation in crops-what did we learn from Arabidopsis? Current Opinion in Biotechnology **32**, 121–129.

Bonnett OT. 1954. The inflorescences of maize. Science **120**, 77–87.

Bradshaw AD. 1965. Evolutionary significance of phenotypic plasticity in plants. Advances in Genetics **23**, 207–215.

Buckley LB, Briones Ortiz BA, Caruso I, John A, Levy O, Meyer A V., Riddell EA, Sakairi Y, Simonis JL. 2023. TrenchR: An R package for modular and accessible microclimate and biophysical ecology. PLoS Climate **2**, e0000139.

Cabrera-Bosquet L, Fournier C, Brichet N, Welcker C, Suard B, Tardieu F. 2016. High-throughput estimation of incident light, light interception and radiation-use efficiency of thousands of plants in a phenotyping platform. The New Phytologist **212**, 269–281.

Choquette NE, Holland JB, Weldekidan T, Drouault J, de Leon N, Flint-Garcia S, Lauter N, Murray SC, Xu W, Wisser RJ. 2023. Environment-specific selection alters flowering-time plasticity and results in pervasive pleiotropic responses in maize. The New Phytologist **238**, 737–749.

Colasanti J, Coneva V. 2009. Mechanisms of floral induction in grasses: Something borrowed, something new. Plant Physiology **149**, 56–62.

Coles ND, McMullen MD, Balint-Kurti PJ, Pratt RC, Holland JB. 2010. Genetic control of photoperiod sensitivity in maize revealed by joint multiple population analysis. Genetics **184**, 799–812.

Cooper M, Tang T, Gho C, Hart T, Hammer G, Messina C. 2020. Integrating genetic gain and gap analysis to predict improvements in crop productivity. Crop Science **60**, 582–604.

Dong Z, Danilevskaya O, Abadie T, Messina C, Coles N, Cooper M. 2012. A gene regulatory network model for floral transition of the shoot apex in maize and its dynamic modeling. PLoS ONE **7**, e43450.

Finlay KW, Wilkinson GN. 1963. The analysis of adaptation in a plant-breeding programme. Australian Journal of Agricultural Research **14**, 742–754.

Flint-Garcia SA, Thuillet AC, Yu J, Pressoir G, Romero SM, Mitchell SE, Doebley J, Kresovich S, Goodman MM, Buckler ES. 2005. Maize association population: A high-resolution platform for quantitative trait locus dissection. Plant Journal **44**, 1054–1064.

Fong Y, Chongzhi D, Huang Y, Gilbert PB. 2017*a*. Model-robust inference for continuous threshold regression models. Biometrics, **73**, 452–462.

Fong Y, Huang Y, Gilbert PB, Permar SR. 2017*b*. chngpt: Threshold regression model estimation and inference. BMC Bioinformatics **18**, 1–7.

Forsythe WC, Rykiel EJ, Stahl RS, Wu H i., Schoolfield RM. 1995. A model comparison for daylength as a function of latitude and day of year. Ecological Modelling **80**, 87–95.

Gaudinier A, Blackman BK. (2020). Evolutionary processes from the perspective of flowering time diversity. The New Phytologist, **225**, 1883–1898.

578 **Guo T, Wei J, Li X, Yu J**. 2023. Environmental context of phenotypic plasticity in flowering time in
579 sorghum and rice. Journal of Experimental Botany **75**, 1004–1015.

580 **Harrison MT, Tardieu F, Dong Z, Messina CD, Hammer GL**. 2014. Characterizing drought stress
581 and trait influence on maize yield under current and future conditions. Global Change Biology **20**, 867–
582 878.

583 **Herrero MP, Johnson RR**. 1981. Drought stress and its effects on maize reproductive systems. Crop
584 Science **21**, 105–110.

585 **Hung HY, Shannon LM, Tian F, *et al.*** 2012. *ZmCCT* and the genetic basis of day-length adaptation
586 underlying the postdomestication spread of maize. Proceedings of the National Academy of Sciences
587 **109,** E1913-E1921.

588 **Itoh H, Nonoue Y, Yano M, Izawa T**. 2010. A pair of floral regulators sets critical day length for
589 *Hd3a* florigen expression in rice. Nature Genetics **42**, 635–638.

590 **Izawa T**. 2021. What is going on with the hormonal control of flowering in plants? Plant Journal **105**,
591 431–445.

592 **Jarquín D, Crossa J, Lacaze X, *et al.*** 2014. A reaction norm model for genomic selection using high-
593 dimensional genomic and environmental data. Theoretical and Applied Genetics **127**, 595–607.

594 **Jin M, Liu H, Liu X, *et al.*** 2023. Complex genetic architecture underlying the plasticity of maize
595 agronomic traits. Plant Communications **4**, 100473.

596 **Johansson M, Staiger D**. 2015. Time to flower: Interplay between photoperiod and the circadian
597 clock. Journal of Experimental Botany **66**, 719–730.

598 **Kiniry JR**. 1991. Maize Phasic Development. In Modeling Plant and Soil Systems (eds J. Hanks and
599 J.T. Ritchie). pp 55–70.

600 **Kiniry JR, Ritchie JT, Musser RL**. 1983*a*. Dynamic nature of the photoperiod response in maize.
601 Agronomy Journal **10**, 10–13.

602 **Kiniry JR, Ritchie JT, Musser RL, Flint EP, Iwig WC**. 1983*b*. The photoperiod sensitive interval
603 in maize. Agronomy Journal **75**, 687–690.

604 **Kusmec A, Srinivasan S, Nettleton D, Schnable PS**. 2017. Distinct genetic architectures for
605 phenotype means and plasticities in *Zea mays*. Nature Plants **3**, 715–723.

606 **Lee SH, Choi CW, Park KM, *et al.*** 2021. Diversification in functions and expressions of soybean
607 *FLOWERING LOCUS T* genes fine-Tune seasonal flowering. Frontiers in Plant Science **12**, 1–16.

608 **Lee JH, Ryu H-S, Chung KS, Posé D, Kim S, Schmid M, Ahn JH**. 2013. Regulation of temperature-
609 responsive flowering by MADS-box transcription factor repressors. Science **342**, 628–632.

610 **Lejeune P, Bernier G**. 1996. Effect of environment on the early steps of ear initiation in maize (*Zea*
611 *mays* L.). Plant, Cell and Environment **19**, 217–224.

612 **McFarland BA, Alkhalifah N, Bohn M, *et al.*** 2020. Maize genomes to fields (G2F): 2014-2017 field
613 seasons: Genotype, phenotype, climatic, soil, and inbred ear image datasets. BMC Research Notes **13**,
614 4–9.

615 **Millet EJ, Kruijer W, Coupel-Ledru A, Alvarez Prado S, Cabrera-Bosquet L, Lacube S,**
616 **Charcosset A, Welcker C, van Eeuwijk F, Tardieu F**. 2019. Genomic prediction of maize yield
617 across European environmental conditions. Nature Genetics **51**, 952–956.

618 **Minow MAA, Ávila LM, Turner K, Ponzoni E, Mascheretti I, Dussault FM, Lukens L, Rossi V,**
619 **Colasanti J**. 2018. Distinct gene networks modulate floral induction of autonomous maize and

This is a provisional file, not the final typeset article

620 photoperiod-dependent teosinte. Journal of Experimental Botany **69**, 2937–2952.

621 **Muller B, Martre P**. 2019. Plant and crop simulation models: Powerful tools to link physiology,
622 genetics, and phenomics. Journal of Experimental Botany **70**, 2339–2344.

623 **Padilla JM, Otegui ME**. 2005. Co-ordination between leaf initiation and leaf appearance in field-
624 grown maize (*Zea mays*): Genotypic differences in response of rates to temperature. Annals of Botany
625 **96**, 997–1007.

626 **Parent B, Tardieu F**. 2012. Temperature responses of developmental processes have not been affected
627 by breeding in different ecological areas for 17 crop species. The New Phytologist **194**, 760–774.

628 **Parent B, Turc O, Gibon Y, Stitt M, Tardieu F**. 2010. Modelling temperature-compensated
629 physiological rates, based on the co-ordination of responses to temperature of developmental processes.
630 Journal of Experimental Botany **61**, 2057–2069.

631 **Rising J, Devineni N**. 2020. Crop switching reduces agricultural losses from climate change in the
632 United States by half under RCP 8.5. Nature Communications **11**, 1–7.

633 **Rogers AR, Dunne JC, Romay C, *et al.*** 2021. The importance of dominance and genotype-by-
634 environment interactions on grain yield variation in a large-scale public cooperative maize experiment.
635 G3: Genes, Genomes, Genetics **11**.

636 **Roof DA**. 1997. Evolutionary Quantitative Genetics. Springer New York, NY

637 **Simpson GG, Dean C**. 2002. Arabidopsis, the Rosetta stone of flowering time ? Science **2002**, 285–
638 289.

639 **Sloat LL, Davis SJ, Gerber JS, Moore FC, Ray DK, West PC, Mueller ND**. 2020. Climate
640 adaptation by crop migration. Nature Communications **11**, 1–9.

641 **Sparks A**. 2018. nasapower: A NASA POWER global meteorology, surface solar energy and
642 climatology data client for R. Journal of Open Source Software **3**, 1035.

643 **Srikanth A, Schmid M**. 2011. Regulation of flowering time: All roads lead to Rome. Cellular and
644 Molecular Life Sciences **68**, 2013–2037.

645 **Swarts K, Gutaker RM, Benz B, *et al.*** 2017. Genomic estimation of complex traits reveals ancient
646 maize adaptation to temperate North America. Science **357**, 512–515.

647 **Teixeira JEC, Weldekidan T, De Leon N, *et al.*** 2015. Hallauer's Tusón: A decade of selection for
648 tropical-to-temperate phenological adaptation in maize. Heredity **114**, 229–240.

649 **Tenaillon MI, Charcosset A**. 2011. A European perspective on maize history. Comptes Rendus
650 Biologies **334**, 221–228.

651 **van Voorn GAK, Boer MP, Truong SH, Friedenberg NA, Gugushvili S, McCormick R, Bustos**
652 **Korts D, Messina CD, van Eeuwijk FA**. 2023. A conceptual framework for the dynamic modeling
653 of time-resolved phenotypes for sets of genotype-environment-management combinations: a model
654 library. Frontiers in Plant Science **14**, 1–14.

655 **Wang E, Engel T**. 1998. Simulation of phenological development of wheat crops. Agricultural
656 Systems **58**, 1–24.

657 **Wang E, Martre P, Zhao Z, *et al.*** 2017. The uncertainty of crop yield projections is reduced by
658 improved temperature response functions. Nature Plants **3**, 1–11.

659 **Wisser RJ, Fang Z, Holland JB, *et al.*** 2019. The genomic basis for short-term evolution of
660 environmental adaptation in maize. Genetics **213**, 1479–1494.

661 **Yang Q, Li Z, Li W, *et al.*** 2013. CACTA-like transposable element in *ZmCCT* attenuated photoperiod

662 sensitivity and accelerated the postdomestication spread of maize. Proceedings of the National
663 Academy of Sciences **110**, 16969–16974.

664 **Zabel F, Müller C, Elliott J, *et al.*** 2021. Large potential for crop production adaptation depends on
665 available future varieties. Global Change Biology **27**, 3870–3882.

This is a provisional file, not the final typeset article

List of Tables and Figures

Table 1. Distribution percentiles for the basic vegetative phase and leaf tip appearance at tassel initiation of panel 1.

Table 2. Impact of latent variable adjustment on PRN-FTP parameter estimation for different maize lines.

Figure 1. Envirotyping of sensed photoperiod across and within maize fields in the Northern Hemisphere.

Figure 2. Adjusting for latent variable effects across a multi-environment trial network when fitting the PRN-FTP.

Figure 3. The PRN-FTP for seven tropical lines of maize.

Figure 4. The trait space for flowering time *per se* and photoperiod sensitivity in a diversity panel of maize.

678 **Table 1. Percentiles of the distribution for the basic vegetative phase at tassel initiation (BVP-ti)**
679 **in panel 1.**

	Min	**5%**	**25%**	**50%**	**75%**	**95%**	**Max**
BVP-ti (ºCd)	183	236	284	320	356	427	499

680

This is a provisional file, not the final typeset article

681 **Table 2. Impact of latent variable adjustment on PRN-FTP parameter estimation for different**
682 **maize lines.**

	Genotype	Intercept (ºCd)	Threshold (h)	Slope (ºCd h^{-1})	RMSE
Unadjusted values					
	CML10	848.3 ± 28.7	12.4 ± 0.7	46.4 ± 10.0	81.6
	CML258	934.1 ± 33.4	12.3 ± 0.7	42.5 ± 11.4	95.2
	CML277	855.8 ± 22.0	14.5 ± 0.6	96.4 ± 18.7	75.4
	CML341	802.1 ± 24.6	12.3 ± 0.6	49.8 ± _8.5	71.4
	CML373	813.9 ± 30.5	12.3 ± 1.1	36.1 ± 10.6	67.3
	Tzi8	855.8 ± 29.5	12.3 ± 1.1	30.2 ± _9.6	86.2
	Tzi9	808.0 ± 29.2	12.2 ± 1.1	26.5 ± _9.2	84.0
Adjusted values					
	CML10	893.3 ± 14.1	14.5 ± 0.6	84.4 ± 12.9	47.9
	CML258	953.1 ± 21.3	12.3 ± 0.9	37.8 ± 7.3	60.7
	CML277	873.7 ± 8.7	14.7 ± 0.6	98.6 ± 8.8	31.3
	CML341	845.0 ± 10.1	14.3 ± 0.6	83.2 ± 7.7	34.8
	CML373	850.7 ± 11.9	12.3 ± 0.8	27.2 ± 4.1	26.2
	Tzi8	888.4 ± 14.8	14.5 ± 1.1	49.0 ± 11.9	53.3
	Tzi9	840.3 ± 11.1	14.4 ± 0.9	42.3 ± 8.7	39.6

683 Root mean squared error (RMSE) is reported for the full bilinear model.

Figure 1. Envirotyping of sensed photoperiod across and within maize fields in the Northern Hemisphere.

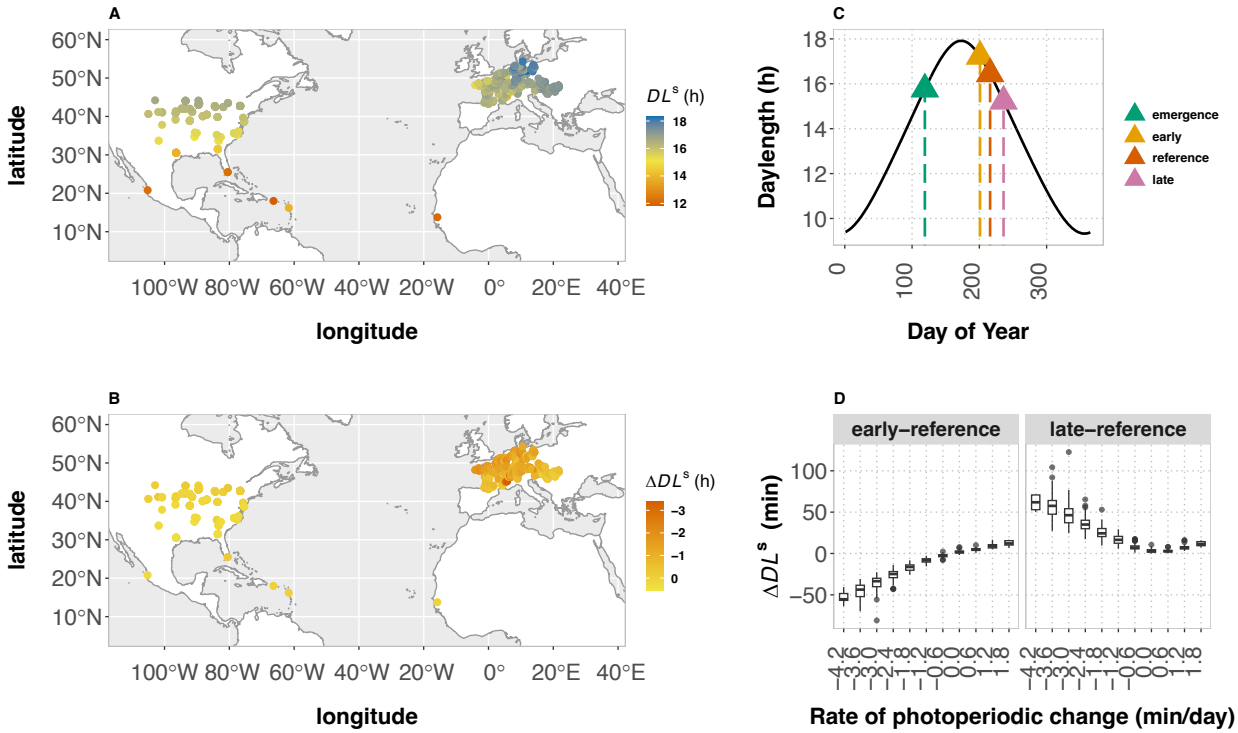

(A) Sensed photoperiod (DL^s for the 50th percentile maturity reference) across maize field sites in the Northern Hemisphere. (B) Within environment differences in hours of sensed daylength (ΔDL^s) between the 95th and 5th percentile maturity groups defined by the BVP-ti distribution of panel 1. (C) The figure portrays how different maturity groups can reach the photoperiod sensitized stage on different days of the year within the same environment, leading to differences in DL^s (the 5th, 50th, and 95th percentile values of the BVP-ti in panel 1are indicated as early, reference, and late maturity groups) (D) The relationship between within environment differences in DL^s and rates of daily photoperiodic change. Here, the differences are shown in minutes for comparisons between the reference maturity group relative to the early and late maturity groups. As reflected in (B), the boxplots show that genotypes within the same environment experience increasingly greater differences in photoperiods when rates of photoperiodic change increase, which occurs in association with increasing latitude.

This is a provisional file, not the final typeset article

Figure 2. Adjusting for latent variable effects across a multi-environment trial network when fitting the PRN-FTP.

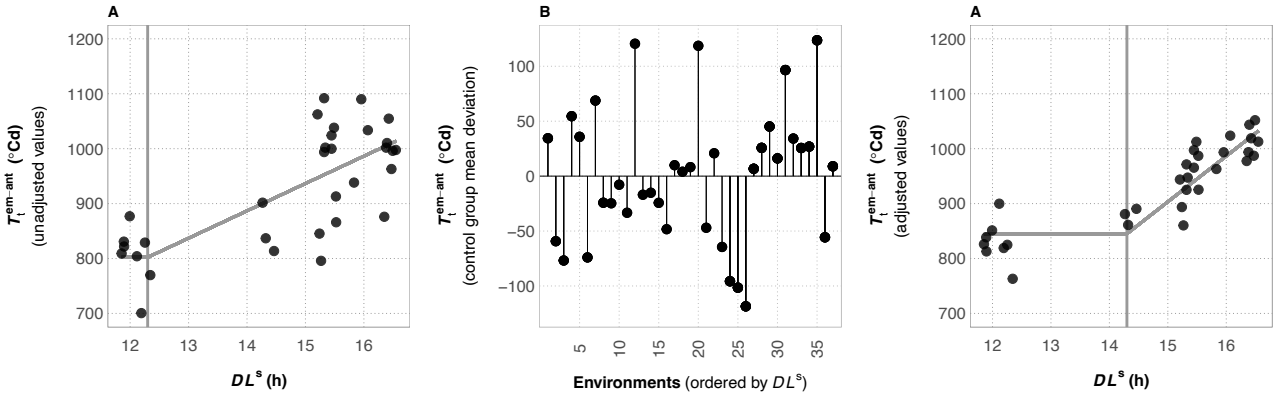

(A) The plot shows the PRN-FTP for genotype CML341, using unadjusted BLUEs for thermal time from crop emergence to anthesis (T_t^{em-ant}; black points). The grey lines show the estimated flowering time *per se* (horizontal line), critical threshold value (vertical line), and photoperiod sensitivity (sloped line). (B) Deviations from the overall average T_t^{em-ant} for the control groups of photoperiod insensitive lines estimated across the same environments, with the environment identifiers ordered as in panels (A) and (B) according to sensed daylength (DL^s). (C) The PRN-FTP for genotype CML341 after adjusting the BLUEs by deviations in (B), leading to different estimates for the flowering time *per se*, the critical threshold value, and the photoperiod sensitivity.

709 **Figure 3. The PRN-FTP for seven tropical lines of maize.**

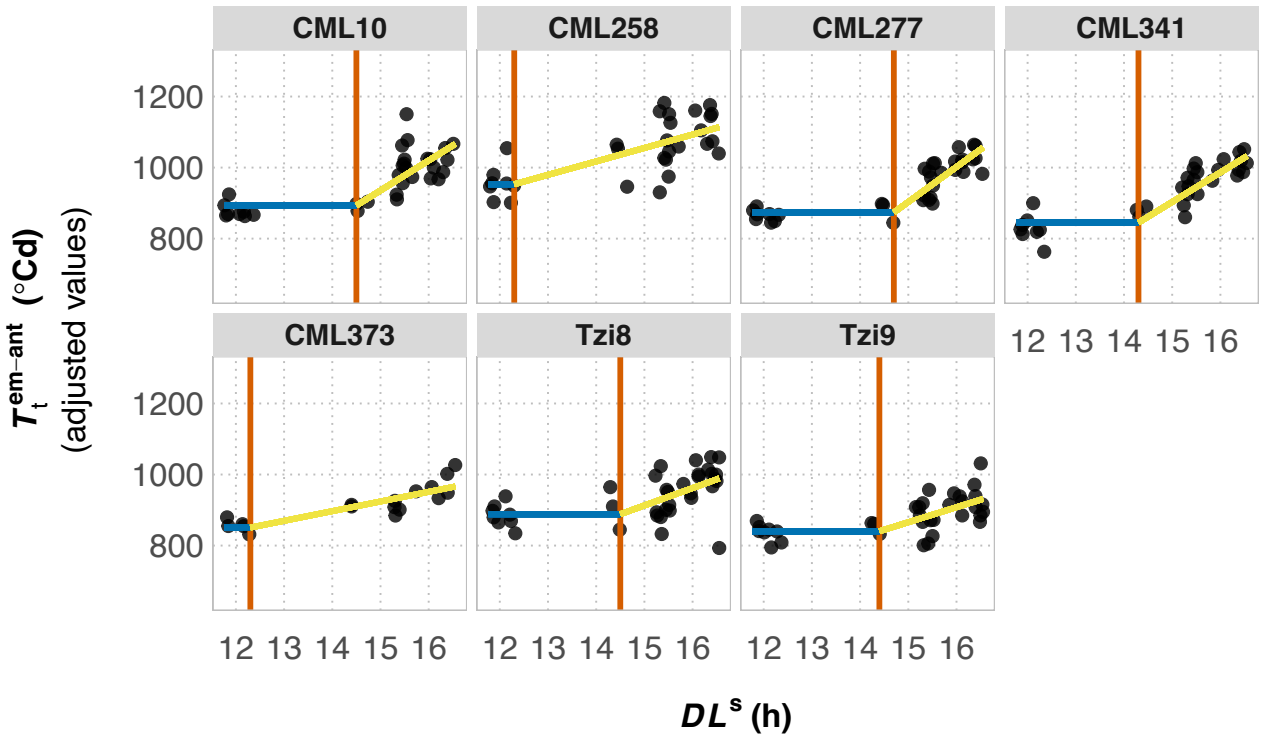

710

711 (A) For each genotype, the plots show the three PRN-FTP parameters estimated from the bilinear
712 function fitted using latent-variable adjusted BLUEs for thermal time from crop emergence to anthesis
713 (T_t^{em-ant}) in relation to sensed daylength (DL^s). Parameter estimates are shown for the flowering time
714 *per se* (blue line), the critical threshold value (red line), and the photoperiod sensitivity (yellow line).

This is a provisional file, not the final typeset article

715 **Figure 4. The trait space for flowering time *per se* and photoperiod sensitivity in a diversity panel**
716 **of maize.**

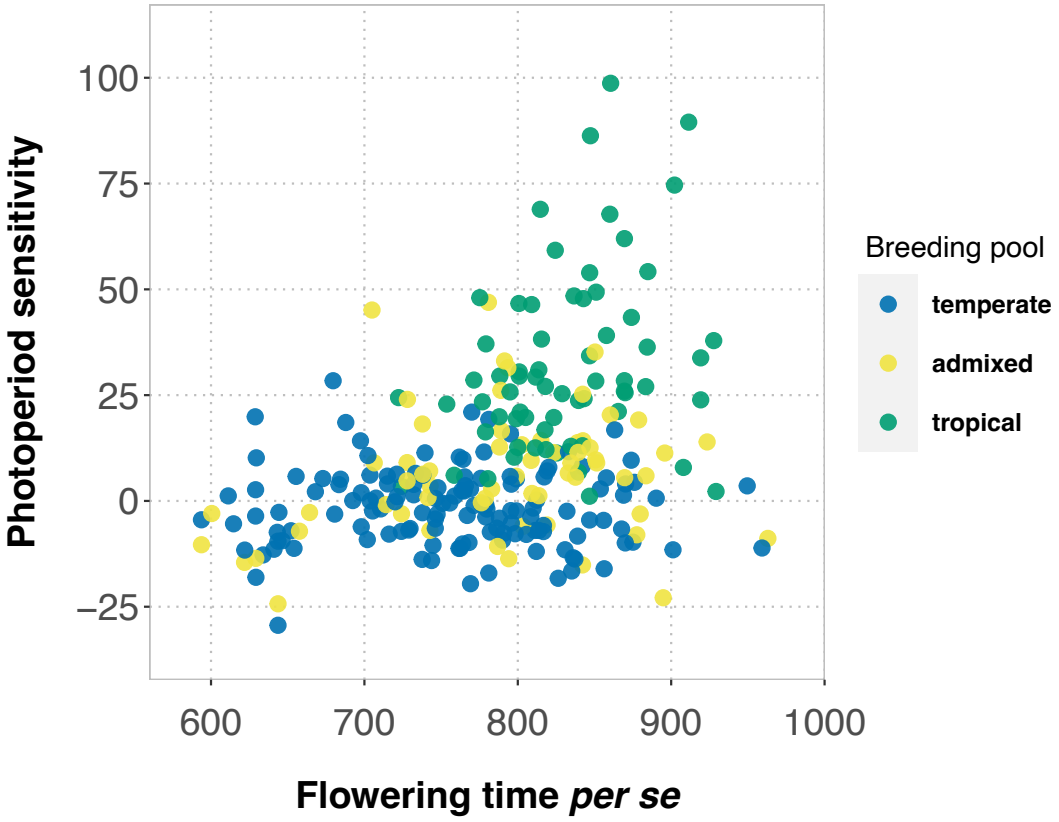

717

718 Points correspond to genotypic values for flowering time *per se* (ºCd) and photoperiod sensitivity (ºCd
719 h^{-1}), estimated using the LD-SD regression method on latent-variable adjusted BLUEs. Breeding pools
720 are represented by samples of inbred lines previously assigned to temperate (*n*=137), admixed (*n*=62),
721 and tropical (*n*=66) sources based on structure analysis of marker data (Flint-Garcia *et al.*, 2005).